MICROSTRUCTURE AND PERFORMANCE OF MICRO CU PILLARS ASSEMBLIES

Mohammed Genanu[1], Babak Arfaei, Ph.D.[5], Eric J.Cotts, Ph.D.[1], Francis Mutuku[2], Eric Perfecto[3], Scott Pollard[4], Aric Shorey[4]

[1]Physics and Materials Science Binghamton University, Binghamton, NY, [2]Universal Instruments Corporation, Conklin, NY, [3]IBM Corporation, Fishkill, NY, USA (now GlobalFoundries), [4]Corning Inc. Corning, NY, USA [5]Ford Motor Company, Ann Arbor, MI, USA

mgenanu1@binghamton.edu

ABSTRACT

The desire for smaller, lighter and faster products drives the development of 2.5D/3D integration technologies that can utilize tens of thousands of connections per die. Micro copper (Cu) pillar geometries have been widely adopted because their small size and fine pitch provides high thermal conductivity, higher input/output (I/O) density and resistance to deleterious electromigration effects. In micro Cu-pillars, SnAg solder is electroplated on top of a Cu pillar. Because of the small volume of solder employed, intermetallic compounds comprise a significant fraction of the resulting solder joint, and very fine Ag_3Sn precipitate morphologies can occur. Thus, the microstructure of SnAg solder/Cu pillar microstructures varies significantly from that of larger solder joints such as flip chip solder joints. Furthermore, 2.5D applications include interposers of distinctly different materials, such as Si or glass. The different properties of these materials such as coefficient of thermal expansion, affect the thermomechanical response of the package to temperature excursions and the lifetime of the package. Thus, behaviors of Cu pillar packages during Accelerated Thermal Cycling (ATC) were examined. Correlations between the shear strength and microstructure of Cu pillars were examined for different solder compositions, and for different aging times. Microstructure analysis (*e.g.* Ag_3Sn precipitate morphology) was performed with both optical and scanning electron microscopy. The effects of thermal aging on the growth of intermetallic compounds (IMCs), the Ag_3Sn precipitate morphology and on the mechanical properties of micro Cu pillar bumps were examined. The shear strength performance of micro Cu pillars with three different bump diameters (30μm, 50μm, and 100μm) was also evaluated. Results were considered in terms of variations in the precipitate morphology, and in terms of increases in the thicknesses of intermetallic layers at micro solder/substrate interfaces. ATC test results for two different interposers (Si and Glass with High CTE) will be discussed.

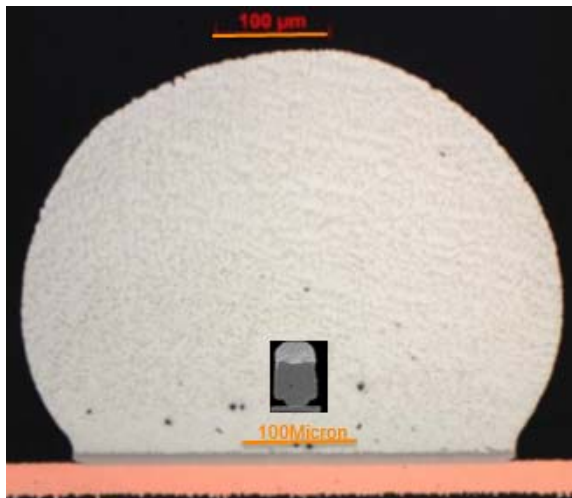Key words: Cu pillars, Lead-Free Solder Alloys, 2.5D Packaging, Interposers, Shear strength

INTRODUCTION

Varying the processing of Pb free solder joints affects their microstructure and their reliability. Important examples are changes in geometry, solder composition or thermal history. Each factor can significantly affect solder joint microstructure and lifetime [1-6]. For instance, the number, size and arrangement of Ag3Sn precipitates each affect the mechanical response of near eutectic Sn-Ag-Cu solder joints, and their reliability [1-8]. Geometry is also an important factor. Smaller solder joints undercool more after reflow and solidify at lower temperatures, generally resulting in a more refined microstructure [9]. Thermal history, most importantly aging time, can also significantly affect Pb free solder joint microstructure and mechanical behavior. Ag3Sn precipitates coarsen during aging and lose their effectiveness in hindering the motion of dislocations, particularly aging at elevated temperatures [10].

In the present study, we seek to better characterize and understand interactions among processing, microstructure and the properties of Pb free, solder joints in Cu pillar geometries. The very large decreases in solder volume realized in Cu pillar solder joint geometries (Fig. 1) would be expected to affect initial microstructures. Changes in solder joint composition and thermal history are correlated with the microstructure, shear strength and accelerated thermal cycling lifetimes of solder joints. The the precipitate morphology are compared with changes in solder composition, and in aging time at elevated temperature. All of these values were correlated to solder joint mechanical properties in an effort to better understand and control determine Cu pillar solder joint reliability. Cu pillars are much stiffer than Pb free solder, resulting in higher stress during assembly processes and in use, with the possibility of reduced reliability, as fracture or delamination may occur. Therefore studies of the mechanical and reliability properties of packaging interconnect Cu pillar joint structures are critical.

The present investigation was focused on the reliability of Si/micro Cu pillar/solder/glass assemblies and Si/micro Cu pillar/solder/Si assemblies, fundamental building blocks of 2.5D packaging. These studies should also be relevant to 3D packaging, where Cu pillars are also utilized. The inclusion

of glass interposers in our study is important, as these materials are important new alternatives to through silicon interposers; glass interposers are relatively stable and low cost, and afford great flexibility in manufacturing arbitrary sizes [7-9]. The investigation used shear strength measurements and accelerated thermal cycling tests to characterize the reliability of silicon/micro Cu pillar/solder/glass assemblies with a wide range of parameter values, including a varied range of pitches. Previous investigations of the shear strength of Cu pillar solder joints have revealed sensitivities to the thickness of intermetallic compounds in the joint, shear speed and shear height [11-30]. This study incorporates these variables and extends such investigations to include careful correlations with solder composition, substrate chemistry and with solder joint microstructure and with results of accelerated thermal cycling tests with assemblies with the same Cu pillar solder joints.

Figure 1. A comparison of microbump (as background) and Cu pillar 30 µm (inset) technologies. Presented on the same scale. The larger aspect ratio of Cu pillar bumps allows finer pitches.

EXPERIMENTAL PROCEDURES
a) Fabrication of Substrate and Chip (Top Die)
The substrates were metallized to allow continuous monitoring of the electrical resistivity of most of the solder joints. The substrate wiring extended beyond the chip area to an array of test probe pads. For both glass and Si interposer substrates, a 0.8 µm SiO_2 / 0.8 µm SiN bilayer was deposited prior to the wiring deposition. A serpentine line was created by alternating lines between the chips and the substrates. The thin film structure consisted of two levels of wiring. The first level, on top of the SiN layer fabricated by electroplating 3 to 4 µm thick Cu lines, either 15 or 20 µm wide, depending on the Cu-pillar pitch. This was followed by a dual dielectric layer of 0.6 µm of SiN and 3 µm of photosensitive PBO dielectric. Then the top layer was deposited as either 7 µm of Cu or 2 µm of Ni/0.08 µm Au on the substrate, or Cu-Pillar structures on the chips.

Si wafers with Cu pillar structures, and both glass and Si interposer substrate, were fabricated at IBM. Three different interposer materials were metallized at IBM, two Corning® glass interposer substrates (one with CTE of 3 ppm/K and one with CTE of 8 ppm/K) and a Si interposer substrate (wafer). Separate Si wafers were fabricated with Cu pillars and solder cap at IBM, in a proven, standard lithography process. The pad diameters were 30, 50 or 100 µm, while the pitch was 90, 140 or 190 µm respectively. Three different Cu pillar heights were produced for each pad diameter (15, 25 or 35 µm). Solder compositions of Sn, Sn0.9%Ag, Sn1.8%Ag and Sn2.4%Ag were deposited at layers of 10 or 20 microns thick (see Table I).

Results were correlated with careful characterizations of microstructure and a wide range of parameter values, including Cu pillar height, aging time, solder and metallization compositions and number of reflows. Different assemblies were fabricated, allowing variation of a number of different parameters, including interposer substrate material, Cu pillar and solder heights and diameters, underbump metallization and solder composition (see Table I).
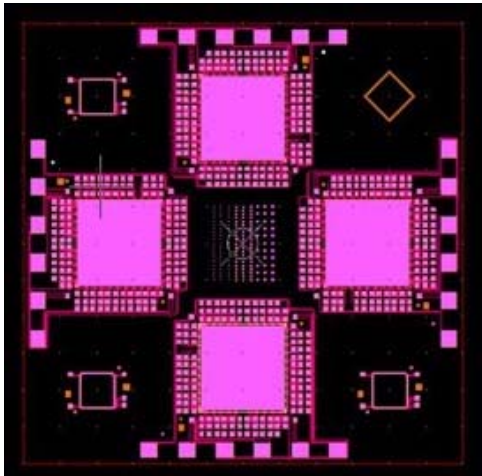
Table 1. Tests parameters in the current study

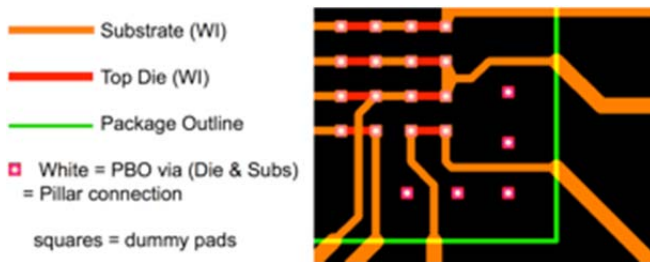| Parameter	Values
Interposer substrate material	Low CTE glass (≈3 ppm/K), High CTE glass (≈8 ppm/K), Silicon
Cu pillar and solder cap heights	25 µm Cu+ 10 µm solder, 15 µm Cu+20 µm solder, 15 µm Cu+ 10 µm solder 35 µm Cu +10 µm solder
Solder cap composition	Sn, Sn0.9%Ag, Sn1.8%Ag, Sn2.4%Ag
Cu pillar pad diameter	30, 50 and 100 µm
Metallization layer, component side	Ni, Cu
Metallization layer, substrate side	Electrolytic Ni/Au, Cu

b) Fabrication of Test Assemblies
Cu pillar assemblies were fabricated at Universal Instruments which included a 60 mm x 60 mm interposer substrate, metallized with a single pad diameter and associated pad pitch in a pattern which accommodated four similar Si 'chips' (each bumped with Cu pillars) (Figures 2 and 3). Cu pillars were dipped in flux and placed on the glass or Si substrate using an automated pick and place machine. Soldering was performed in a forced convection reflow oven with a nitrogen atmosphere. Peak solder joint temperature during the reflow process was measured on a setup board to be between 240 and 245 degrees Celsius and time above liquidus was 64s. After reflow all assemblies were inspected electrically using an ohm-meter and through x-ray imaging (X-ray imaging itself was not sufficient to reveal an acceptable solder joint formation during the

assembly process due to small size of joints). The design allowed the electrical continuity of most of the solder joints (including the corner joints) to be continuously monitored during ATC test. As seen in Figure 2, the substrates were designed to be tested in multiples of four testable units.

Figure 2. Test assemblies were built using SMT process, with four similar Si 12 x 12 mm 'chips' (with Cu pillars) placed on Si or glass substrates (60 x 60 mm).

Figure 3. Detail of the assembly at the corner of the package ('chip' with Cu pillars) from Fig. 2. The design allowed the electrical continuity of most of the solder joints (including the corner joints) to be continuously monitored during ATC test.

c) Microstructure Characterization

Samples were mounted in epoxy for metallographic sectioning after reflow and after reliability test. Also Cu pillar samples (chip) and substrate (both glass and Si) were analyzed. All the samples were ground in a series of steps with abrasive paper, polishing cloths with diamond suspension, and finally with a 0.02 μm colloidal silica suspension. Great care was used with each polishing step to remove as much damage as possible from the previous polishing step. With the final polishing step, the goal was to have no polishing damage, (neither scratches nor crystal deformation), left in the Sn as a result of specimen preparation.

The specimens were imaged using an optical metallography, in both Bright Field (BF) imaging and polarized light with the polarizers nearly crossed (cross polarizer (XP) imaging). The XP imaging contrast in Sn arose from the birefringent properties of Sn, leading to different colors for different
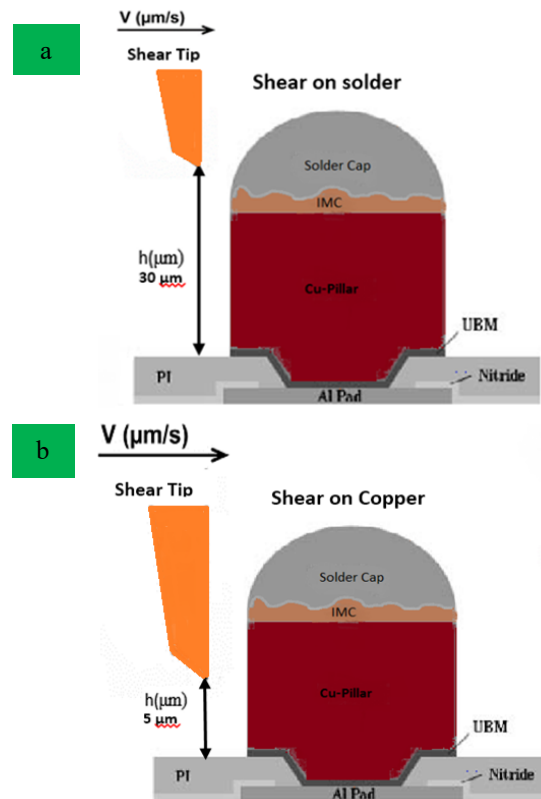
crystal orientations of Sn under XP imaging [31]. Selected specimens were imaged using a SEM. Images were taken using backscatter electron (BSE) imaging. In BSE composition mode images, contrast is proportional to the average atomic number of the material.
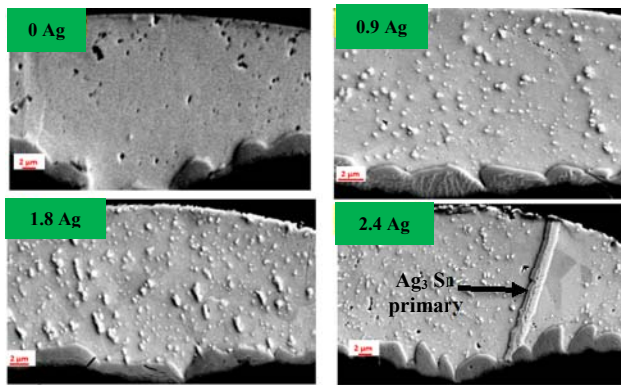
d) Measurements of Shear Strength

The shear strength tests were conducted using a DAGE-SERIES-4000 Plus bond tester. The shear loading speed was 700 μm/s (with a maximum test load of 400 g) (Fig. 4), in accordance with the JEDEC JESD22-B117A standard [32, 33]. Measurements done at room temperatures were repeated on multiple nominally identical samples. The dependence of shear strength on system parameters (e.g., solder composition, size and aging time), and on shear strength measurement parameters as shear height, was examined. Shear test was performed on both Cu pillar and on solder cap.

e) Accelerated Thermal Cycling Test

Accelerated thermal cycling (ATC) test was performed at Universal Instruments Corporation. A -40/125°C ATC test was utilized with 15 minute dwell times at the temperature extremes and 9°C per minute transition rates between the extremes, consistent with IPC-9701 criteria [34]. A solder joint failure was defined when the resistance of the joint exceeded 900 ohms. Generally, after failure was detected, samples were removed from the chamber for microstructural characterization.

Figure 4. Schematics of low speed shear test. Shear test was performed on both (a) solder cap (b) and Cu pillar [33].

Figure 5. SEM micrographs of Cu pillars pad diameters of 100 μm with different solder compositions, as noted in the figure on the Si chip. The Ag$_3$Sn precipitate morphology was observed to change with Ag composition in the solder.
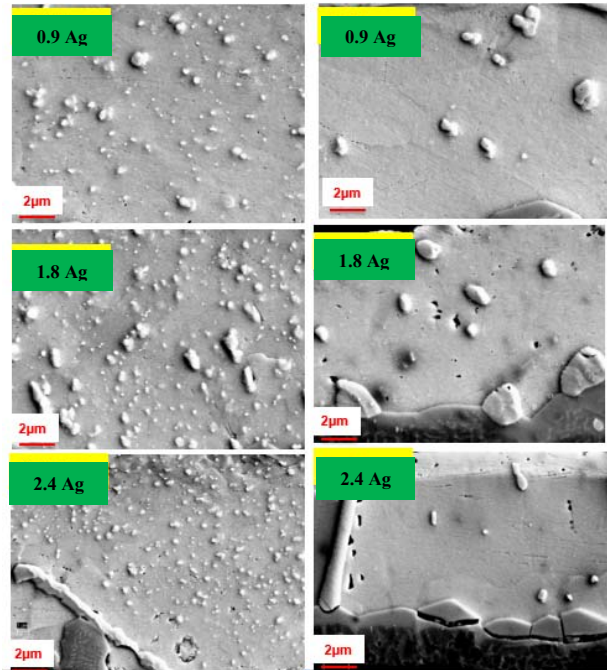
RESULTS

The effect of composition and aging on the microstructure and shear strength of Cu pillar solder joints was examined. The microstructure of the solder joint was evaluated in the as-fabricated configuration, and after aging. Varying the solder composition or the thermal history of SnAg or SnAgCu solder joints affects their microstructure and their mechanical response. [1-6] The number, size and arrangement of Ag$_3$Sn precipitates affect the mechanical response of Sn-Ag-Cu near eutectic solder joints, and their reliability.[1–8] A large number of fine Ag$_3$Sn precipitates (Fig. 5) would be expected to be much stronger than one with a few, large Ag$_3$Sn precipitates (Fig. 6, micrographs for aged samples). A number of different thermal history parameters influence the Sn-Ag-Cu microstructure, including aging time. A fine Ag$_3$Sn precipitate morphology in Sn-Ag-Cu solder (such as that of Fig. 5) will coarsen over time, particularly at elevated temperatures, and the mechanical properties of the solder would be expected to change. These effects were examined for Cu pillar solder joints before and after aging.
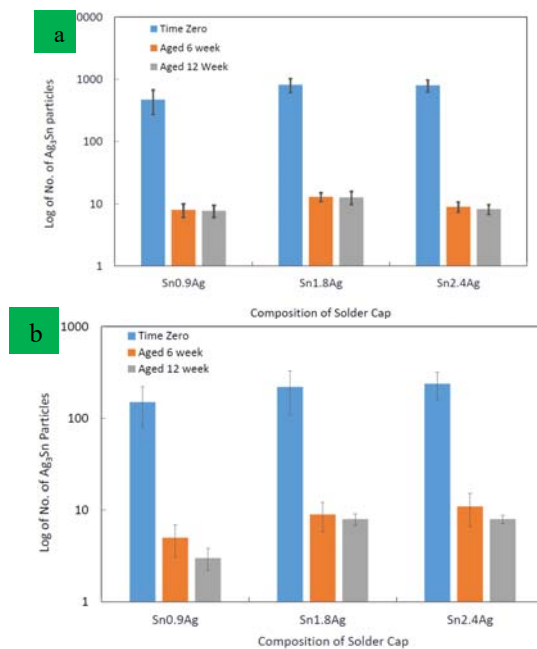
The effect of Ag concentration on the microstructure of Cu pillar/SnAg solder joints is illustrated in Fig. 5. A number of Ag$_3$Sn precipitates are seen in all of the joints containing Ag, even for the solder joint with solder containing 0.9%Ag. The spacing between precipitates ranged from 0.1 μm to approximately 2 μm, with more submicron spacings for the solder joint containing 2.4%Ag (Fig. 5). Such fine spacings between Ag$_3$Sn precipitates were observed at essentially all points in the Sn matrix of the Cu pillar solder joints. In contrast to larger Pb free solder joints (see for example Fig. 1), where recalescence causes much of the joint to solidify at or near the melting temperature of the alloy, these much smaller Cu pillar solder joints would not increase in temperature as much after initial solidification. Thus a more homogeneous distribution of fine precipitates would be expected to be observed (Fig. 5 and Fig. 6).

Aging these Cu pillar solder joints resulted in a dramatic decreases in the number of Ag$_3$Sn precipitates in the solder joint. Aging was conducted at a temperature of 125°C for a period of 1000h, resulting in significant coarsening of the precipitates (Fig. 6). The number of precipitates in a cross section of a typical solder joint decreased from several hundred to less than ten for all Ag concentrations (Figs. 7).
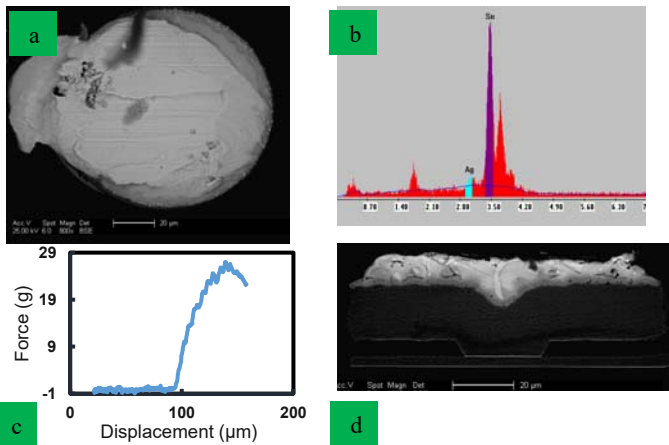

Figure 6. Backscattered SEM images of two category Cu pillars on the left after reflow. The right is after 1000 hour (6 weeks) of aging at 125°C. The number of Ag$_3$Sn precipitates have decreased while their size is increased. Pad diameter of pillars is 30μm on the Si chip.

Figure 7. The quantititave analysis for the number of the Ag$_3$Sn preciptitates as function for aging time (a) Pad diameter 100 μm (b) Pad diameter 30 μm
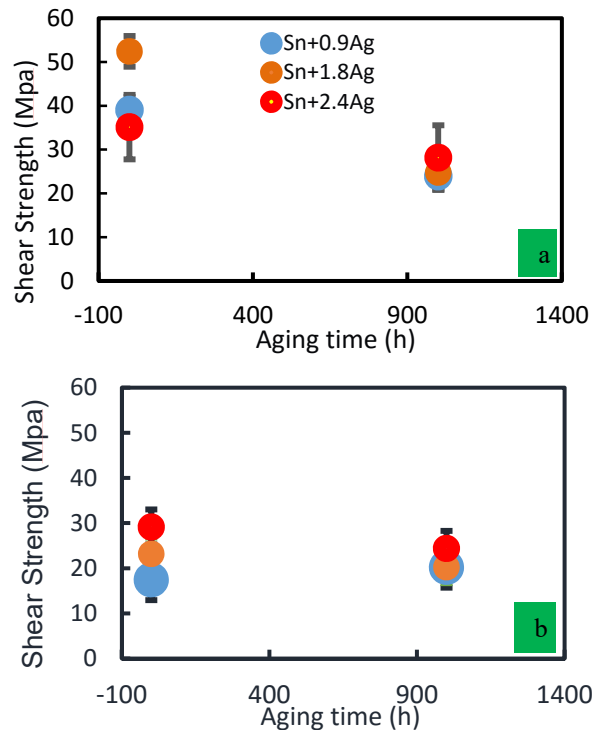
Figure 8. Shear strength of solder cap after 1000 h aging (a) top view for the failure for sample with pad diameter 30 μm, (b) EDX to prove the failure type, (c) force-displacement for pad diameter 100 μm, (d) cross-section after failure for sample with pad diameter 100 μm on Si chip.

Measurements of shear strength conducted on Cu pillar/SnAg solder joints, so as to examine, separately, the shear strength of the Cu pillar and of the solder. Examination of the metal remaining on the pad after shearing using scanning electron microscopy, Fig. 8(a) and energy dispersive analysis, Fig. 8(b), along with plots of the force versus displacement, Fig. 8(c) provided insight on the nature of the failure in the solder joint. If the force versus displacement plot indicated ductile failure (e.g. Fig. 8(c)), and the majority of the remaining metal on the pad was Sn (e.g. Fig. 8(b)), then the indication was ductile failure in the solder. This was confirmed in the present case by scanning electron microscopy micrograph of a cross section of the shear solder joint (Fig. 8(d)), which revealed a significant amount of solder remaining on the pad. Solder failure was observed to be ductile for all samples tested, including all compositions, as reflowed and aged samples, for both pad diameters.
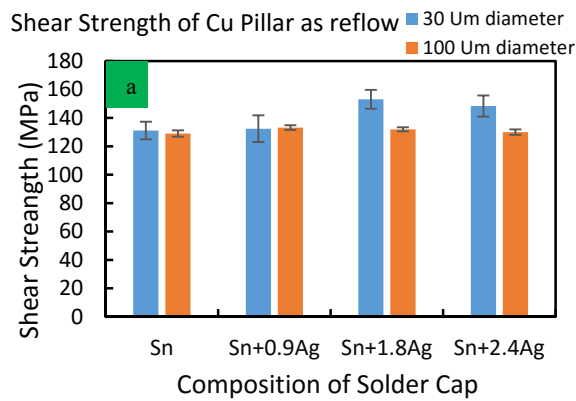
Measurements of shear strength were conducted for a variety of Cu pillar/solder joints, both as reflowed and after 1000h of aging at a temperature of 125°C (Fig.9). Three different solder compositions were studied, with different Ag concentrations, and two different Cu pillar diameters were examined, 30 and 100 micron. After aging, the values for shear strength were essentially the same for all samples, with values near to 23 MPa. This correlated with the observation that the Ag3Sn precipitates had coarsened significantly in all of the samples after aging, leaving few (less than ten) precipitates in a given cross section. The spacing between precipitates was approximately 10 μm, so the precipitates no longer significantly hindered dislocation movement. In 30 micron diameter Cu pillars, the shear strength of as received samples was generally significantly higher than that for aged samples, with Sn1.8Ag samples exhibiting values above 50 MPa, compared to approximately 38MPa for Sn0.9Ag samples. Lower values of shear strength for Sn2.4Ag samples may reflect the

possibility of formation of primary Ag3Sn precipitates in these samples, thus decreasing the Ag available for the fine, secondary Ag3Sn precipitates (Fig. 5 and Fig. 6). But counts of numbers of secondary Ag3Sn precipitates in these samples were similar to those for Sn1.8Ag solder joints (Fig. 7). Values of the shear strength of as reflowed, 100 μm diameter Cu pillar solder joints were distinctly lower than for the 30 μm diameter Cu pillar solder joints (Fig. 9), values were close to those of the aged solder joints. This despite a similar spacing between Ag3Sn precipitates in both as received 100 μm and 30 μm Cu pillar SnAg solder joints.

Figure 9. Shear strength of solder cap depending on solder composition and pad diameter (solder volume) for (a) pad diametere 30 μm, and (b) pad diametere 100 μm.
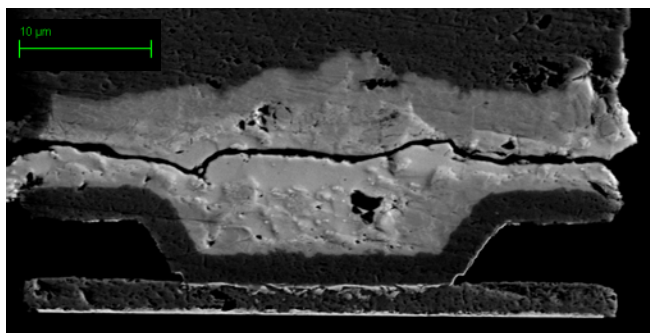
Shear strength measurements were conducted for the Cu pillars themselves (Fig. 4 (b)), in an effort to examine the relative strength of the Cu pillar and the Al pad/pillar bond. The results revealed the strength of the Cu pillar/Al pad bond, as all failures were observed to be in the Cu pillars (e.g. Fig. 10(b)). Values for the shear strength of Cu pillars themselves were all similar in the as fabricated state; shear strengths of 130 MPa were observed (Fig.10-a).

Figure 10. (a) The shear strength of the pillars after reflow, (b) the optical micrographs showing the failure of the pillar after shearing.

Accelerated thermal cycling (ATC) between -40°C and 125°C was conducted to characterize the interconnect reliability of the Cu pillar non underfilled assemblies. Comparisons were made between the performance of Si/high CTE glass interposer assemblies and Si/Si interposer assemblies. These Cu pillar assemblies had fifty μm diameter Cu pillars, and Sn1.8Ag solder.
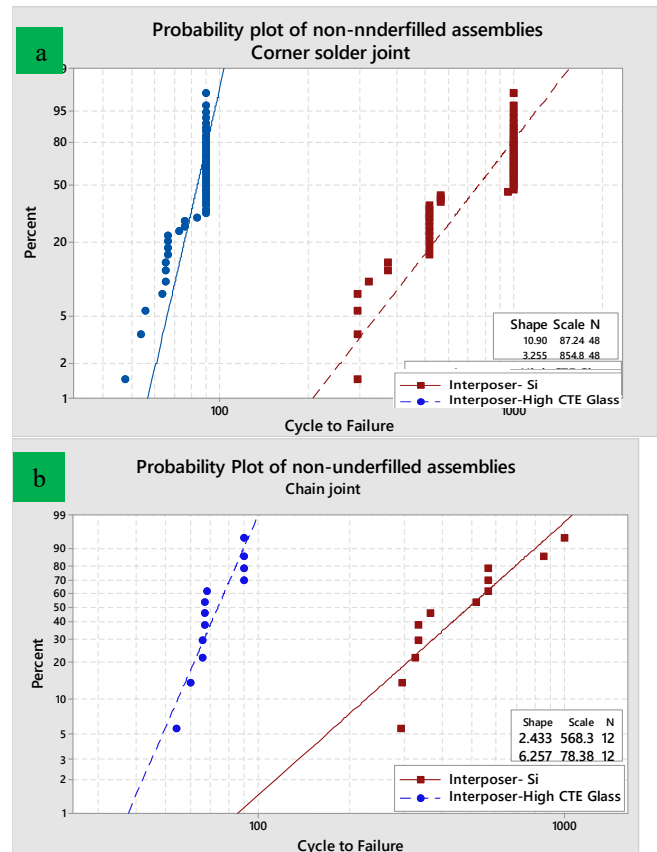
Failure of the Cu pillar solder joints was observed to occur via crack propagation through a relatively thin solder layer remaining between intermetallic compounds after assembly and ATC testing (e.g. Fig. 11). Such a failure was similar to those observed in more conventional surface mount geometries, such as CSPs [24]. Similar results were found for both corner and chained end joints (Fig. 12).

Figure 11. Backscattered SEM images of a failed sample after ATC test of with cycles between -40°C and 125°C. Failure was observed in the remaining solder. The solder composition was Sn-1.8Ag and pad diameter was 50 μm with Si interposer.

These ATC results are presented in Fig. 12 in the form of two parameter Weibull plots of cumulative percentage of failures (percent) versus number of cycles before failure. Fits to these data sets provided estimates of the shape parameter (slope), β and characteristic lifetime (scale), η for each data set. Lifetimes were more than an order of magnitude larger for the Si/Si assemblies than for the Si/high CTE interposer assemblies (Fig. 12).

Figure 12. Weibull distribution of lifetime (a) corner joints of non-underfilled assemblies, (b)chain joints non-underfilled high.

CONCLUSIONS

In the current study, relations between processing, microstructure and reliability of assemblies enabled through Cu pillar/interposer technology were examined. Both Si/micro Cu pillar/solder cap/glass and Si/micro Cu pillar/solder cap/Si assemblies with a large number of I/Os were examined in a configuration that allowed monitoring of electrical continuity during test. Significant variation in Ag$_3$Sn precipitate morphology was observed under nominally identical fabrication conditions. These were correlated with relatively large variations in mechanical behavior, for instance in measured values of shear strength. Large variations in Ag$_3$Sn precipitate size and number were also observed with changes in composition and upon aging, as would be expected. Cu pillar assemblies revealed small, but continuous solder layers. After failure during ATC, cracks were found to have propagated through these continuous solder layers. Even though the Si to Si joint have no CTE mis-match there were still solder fails and so

underfill is recommended for all structures, both Si-Si and Si-glass will benefit.

ACKNOWLEDGEMENTS

REFERENCES

[1] A. Lee, T. K. , Bieler, Th. R., Kim, C. U. , Ma, H "Fundamentals of Lead-Free Solder Interconnect Technology from Microstructures to Reliability" (Springer, 2015, New York)

[2] Puttlitz, K. J. and Stalter, K. A. "Handbook of Lead-Free Solder Technology for Microelectronic Assemblies" (CRC Press, 2004)

[3] M. Sona and K. N. Prabu, J. Mater. Sci. 24, 3149 (2013).

[4] H. R. Kotadia, P. D. Howes, S. H. Mannan, Micro. Rel. 54, 1253(2014).

[5] P. D. Pereira, J. E. Spinelli, A. Garcia, Mat. and Design, 45, 377 (2013).

[6] S. L. Allen, M. R. Notis, R. R. Chromik, and R. P. Vinci, J. Mater. Res. 19, 1417(2004).

[7] M. Kerr, N. Chawla, Acta Materialia, 52, 4527 (2004).

[8] M. Lu, D. Y. Shih, P. Lauro, C. Goldsmith, D. W. Henderson., Applied Physics Letters, 92:211909 (2008).

[9] G. Parks, B. Arfaei, M. Benedict, E. Cotts, M Lu, E. Perfecto," The dependence of the Sn grain structure of Pb-free solder joints on composition and geometry", *Proc. 62nd Electronic Components and Technology Conference (ECTC)*, pp. 703-709, May. 2012.

[10] B. Arfaei B., N. Kim, E.J Cotts., "Dependence of Sn Grain Morphology of Sn-Ag-Cu Solder on Solidification Temperature", *Journal of Electronic Materials*, vol. 41, no. 2, pp. 362-374, 2012.

[11] Y. H. Ko, M.S. Kim, J. Bang,T.S. Kim, C.W. Lee, "Properties and Reliability of Solder Microbump Joints Between Si Chips and a Flexible Substrate" Journal of ELECTRONIC MATERIALS, Vol. 44, No. 7, 2015. pp. 2458-2466.

[12] J. Bertheau. Et al., "Effect of intermetallic compound thickness on shear strength of 25 mm diameter Cu-pillars" Intermetallics Vol. 51, 2014, pp. 37- 47.

[13] A. Shorey, S. Pollard, A Streltsov, G. Piech, R. Wagner, Electronic Components and Technology Conference (ECTC), IEEE 62nd , May 2012.

[14] T. Wang, F. Tung, L. Foo and V. Dutta, "Studies on A novel flip-chip interconnect structure – pillar bump," IEEE Conference Publications, 2001 Proceedings 2001, pp.933-937.

[15] E. Perfecto, Flip Chip Fabrication and Interconnection Course, Electronic Components and Technology Conference, 2015.

[16] M. Huang, G. Y. Ong, Y. P. Chia, and T. Jiang, "Intermetallic formation of copper pillar with Sn-Ag-Cu for flip-chip-on-module packaging," IEEE Trans. Compon. Packag. Technol., vol. 31, no. 4, pp. 767-775, Dec. 2008.

[17] K. M. Chen and T. S. Lin, "Copper pillar bump design optimization for lead free flip-chip packaging," J. Mater. Sci, Mater. Electron., vol. 21, no. 3, pp. 278–284, Mar.2010.

[18] J. R. Jhou, M. Y. Tsai, C . Y. Wu, and K. M . Chen, "Thermal stresses and deformations of Cu pillar flip chip BGA package: Analyses and measurements," 2010 5th International Microsystems Packaging Assembly and Circuits Technology Conference

[19] S. Movva, et al,"Cu-BOL(Cu-column on BOL) technology: A low cost flip chip solution scalable to high I/O density, Fine Bump Pitch and advanced Si-nodes," Electronic Components and Technology Conference, May 2011.

[20] L. Minjae et al., " Study of Interconnection Process for Fine Pitch Flip Chip" ECTC 2009. pp. 720-723.

[21] Y.J. Chen, C.K. Chung, C.R. Yang, C.R. Kao, "Single-joint shear strength of micro Cu pillar solder bumps with different amounts of intermetallics," Microelectron Reliability, vol.53, 2012, pp.47-52

[22] B. Lin, T. Gregorich " Design and Characterization of a Copper-Pillar Flip Chip Test Vehicle for Small Form-Factor Packages Using 28nm ELK Die and Bump-On-Trace (BOT)" IEEE pp. 218-221

[23] A. Shorey, J. Keech, S. Pollard, P. Cochet , K. Ruhmer, A. Huffman M. Lueck, "Advancements in Fabrication of Glass Interposers" Electronic Components and Technology Conference, ECTC 2014. 64th, May 2014.

[24] H.Y.Son, et. at. "Thermal cycling reliability of Cu/SnAg double-bump flip chip assemblies for 100 μm pitch applications" JOURNAL OF APPLIED PHYSICS. Vol. 105, No. 013522. 2009. p. 105.

[25] B. Kim, G. Lim, J. Kim, K. Lee, Y. Park, H. Lee, Y. Joo, "Intermetallic compound growth and reliability of Cu pillar bumps under current stressing," Journal of electronic materials, Vol. 39, No. 10, 2010.

[26] B.H. Kwak, M.H. Jeong, J.W. Kim, H.J. Lee, Y. B. Park, "Correlations between interfacial reactions and bonding strengths of Cu/Sn/Cu pillar bump," Microelectronic Engineering, vol.89, 2012, pp.65-69.

[27] C. R. Kao, A. T. Wu, K. N. Tu, Y. Lai, "Reliability of micro-interconnects in 3D IC packages" Microelectronic Reliability, v53 no.1, pp 1- 182, 2013.

[28] K. Suganuma. K., 2011, "Advances in lead-free electronics soldering. Current Opinion in Solid State and Materials Science," vol.5, no.1, 2001, pp.55-64.

[29] H. Zhang, E. Perfecto ; V. L Calero-DdelC ; F. Pompeo "An Effective Method for Full Solder Intermetallic Compound Formation and Kirkendall Void Control in Sn-base Solder Micro-joint, Electronic Components and Technology Conference, May 2015, pp 1695-1700.

[30] F. Mutuku, B. Arfaei, E.J Cotts "Effect of variation in the reflow profile on the microstructure of near eutectic SnAgCu alloys" May, 2014 IEEE 64th Electronic Components and Technology Conference (ECTC).

[31] B. Arfaei, M. Benedict, E. J. Cotts, "Nucleation rates of Sn in undercooled Sn-Ag-Cu flip-chip solder joints," Journal of Applied Physics , vol.114, no.17, pp.,173506-10, 2013"

[32] JEDEC Standard, "Solder Ball Shear", JESD22-B117A, October 2006.

[33] Mohammed Genanu, B. Arfaei, F. Mutuku, E. J. Cotts, Eric Perfecto, Scott Pollard, Aric Shorey "Reliability Assessment and Microstructure Characterization of Cu Pillars Assembled on Si and Glass Substrates " June, 2016 IEEE 66th Electronic Components and Technology Conference (ECTC).

[34] IPC-9701A "Performance Test Methods and Qualification Requirements for Surface Mount Solder Attachments"